ACS EARTH AND SPACE CHEMISTRY

http://pubs.acs.org/journal/aesccq

Article

Incorporation of Ambient Water-H into the C-Bonded H Pool of Bacteria during Substrate-Specific Metabolism

Arnim Kessler, Stefan Merseburger, Andreas Kappler, Wolfgang Wilcke, and Yvonne Oelmann*

Cite This: *ACS Earth Space Chem.* 2022, 6, 2180−2189

Read Online

ACCESS | Metrics & More | Article Recommendations | Supporting Information

ABSTRACT: The stable isotope ratios of C-bonded H (δ^2H_n values) can be used to locate soil samples for forensic purposes because of their close correlation with the δ^2H values of precipitation. Post-sampling bacterial activity might change the δ^2H_n values via glycolysis. We tested to which degree C-bonded H is replaced by H from ambient water under favorable and unfavorable growing conditions. We provided two heterotrophic bacteria (*Bacillus atrophaeus*, *Escherichia coli*) with glucose (favorable) or lysine (unfavorable) under aerobic conditions. We assessed the H incorporation from ambient water via ^2H labeling. We found that the H incorporation into bacterial biomass in the glucose treatment was 79 ± 5.9% (*B. atrophaeus*) and 43 ± 3.0% (*E. coli*), likely as a consequence of glycolysis and conservation of the δ^2H value in the anabolic mode of the tricarboxylic acid (TCA) cycle. Differences between species were possibly related with different compositions of metabolite mixtures. The bacteria did hardly grow with lysine while respiration continued, and we found no H incorporation because the catabolic mode of the TCA cycle, which was active when the bacteria grew on lysine, is associated with CO_2 release and a complete cleavage of former C−^2H bonds. Our results support the glycolysis pathway as a mechanism underlying the incorporation of ambient-water H into the C-bonded H pool of bacteria. Stressful conditions forcing bacteria into a catabolism-dominated metabolism disable the incorporation of ambient-water H, and δ^2H_n values can be applied to identify the origin of soil samples in forensics.

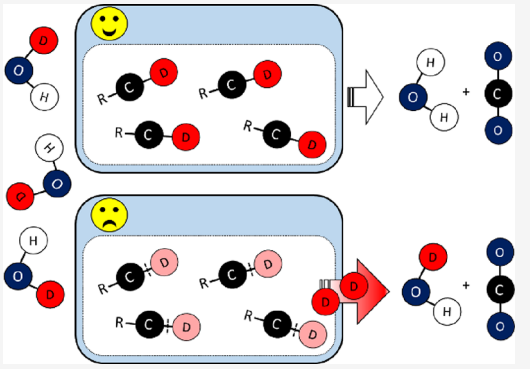

KEYWORDS: *stable H isotopes, C-bonded H, incubation, glucose, lysine*

INTRODUCTION

Stable H isotope ratios (δ^2H values) of carbon (C)-bonded H in compounds formed during young age and conserved for the whole life can help identify the region of birth of humans[1] or the natal origin of migrating animals.[2−4] The stable H isotope approach is based on the reliance of organisms on regional water sources with typical geographical patterns in δ^2H values.[5] Similarly, δ^2H values of C-bonded H (δ^2H_n) of soil organic matter (SOM) that is built up from organismic remains correlates closely with δ^2H values of precipitation.[6,7] Therefore, the origin of soil samples, which can be required, e.g., as evidence in criminal cases, might be deducible from δ^2H_n values of SOM. However, not only dead organic remains with a preserved δ^2H_n value but also living microorganisms including bacteria are present in soil. Because of the short life cycle of bacteria of minutes to hours, no long-lived tissue exists in living bacterial cells and the δ^2H_n values can be quickly metabolically overprinted by the introduction of H atoms from ambient water.[8,9]

It is generally assumed that during glycolysis, a metabolic reaction chain shared by nearly all organisms on Earth,[10] ambient-water H is incorporated into the C-bonded H fraction which includes *de novo* formation of C−H bonds.[11−15] During the fifth step of the glycolysis, an H atom from ambient water is newly bound to the C_2 position of the glycerinealdehyde-3-phosphate (GAP) molecule. This H atom is eventually conserved in bacterial biomass if pyruvate as the end-product of glycolysis enters the anabolic mode of the tricarboxylic acid (TCA) cycle that generates biosynthesis products. Because many bacteria prefer glucose, the educt of the glycolysis, as a C source[16] for biosynthesis, an incorporation of ambient-water H was found if *Escherichia coli* or *Bacillus subtilis* were grown on glucose or growth substrates amended with glucose.[8,17] In these studies, the incorporation of ambient-water H was calculated for the bulk bacterial biomass.[8,17] Bulk bacterial biomass consists of both C-bonded H as well as O-, N-, and S-bonded H (exchangeable H; H_{ex}) that rapidly exchanges with ambient air moisture, e.g., in the laboratory atmosphere.[18,19] Therefore, the calculation of incorporation of ambient-water H in previous

Received: March 23, 2022
Revised: July 7, 2022
Accepted: August 4, 2022
Published: August 18, 2022

https://doi.org/10.1021/acsearthspacechem.2c00085
ACS Earth Space Chem. 2022, 6, 2180−2189

studies on bacteria did not relate exclusively to C-bonded H. Accordingly, the calculated ambient-water H incorporation into bacterial biomass of up to 30% of total H[8,9,20,21] and of <5 to >70% into bacterial amino acids[17] contains uncertainties. The quantification of the incorporation of ambient water-H into bulk bacterial biomass requires distinguishing between exchangeable and nonexchangeable H which can be reached by steam equilibration.[19,22] However, this method has not been applied in microbiological studies so far.

Jointly, *de novo* formation of C−H bonds during glycolysis and the incorporation of ambient-water H during bacterial metabolism might suggest that H in the newly formed C−H bonds originates from cell water reflecting ambient water. However, the role of glycolysis for the incorporation of ambient-water H during bacterial metabolism has not been studied yet. Most bacterial species cannot grow on substrates that are not involved in glycolysis e.g., lysine, a ketogenic amino acid.[23−25] However, as an adaption to stationary phase growth condition, *E. coli* was shown to continue metabolic activity including the gluconeogenesis/glycolysis pathways if provided with lysine.[25] Knorr et al.[25] showed that *E. coli* is able to degrade lysine catabolically. However, the used incubation medium was supplemented with glucose resulting in basic glycolytic activity and does not provide information about bacterial growth and incorporation of ambient water-H when lysine is the sole C-source.

The incorporation of ambient-water H into biosynthesized compounds is associated with enzymatically mediated reactions which fractionate H and thus produce kinetic isotope fractionation.[26−28] As opposed to different isotope fractionations during the biosynthesis of individual bacterial lipids,[29−32] bulk bacterial biomass should be characterized by a consistent fractionation factor if glycolysis precedes the majority of biosynthesis products. For bacterial biomass and spores, a range of net apparent fractionation ($\varepsilon_{\text{biosynthesis product/water}}$) from +40 to +122 ‰ was reported.[20] However, the study of Kreuzer-Martin et al.[20] did not compare different bacterial species and thus, does not allow to draw conclusions on a consistent fractionation factor irrespective of bacterial species.

We aimed to prove that ambient-water H is incorporated into C-bonded H during glycolysis. Moreover, we aimed to quantify the apparent H isotope fractionation by this H incorporation. We hypothesized that (i) there will be pronounced growth and a substantial incorporation of ambient-water H in the glucose treatment irrespective of the bacterial species; (ii) in the lysine treatment, *E. coli* will show metabolic activity and associated incorporation of ambient water-H into C-bonded H, whereas *B. atrophaeus* will die; and (iii), the isotope fractionation associated with the incorporation of ambient-water H into bulk bacterial biomass in the glucose treatment will be constant, i.e., not depend on the bacterial species.

MATERIAL AND METHODS

Bacterial Cultures and Medium Preparation. No unexpected or unusually high safety risks arose during the experiment. We used the Gram-positive bacterium *Bacillus atrophaeus* (DSM 675) and the Gram-negative bacterium *Escherichia coli* K-12 (MG 1655) (DSMZ, Braunschweig, Germany). Cultures were pre-grown in a Luria-Bertani (LB) medium at pH 7. Afterward, *E. coli* and *B. atrophaeus* cultures were inoculated and incubated in Erlenmeyer flasks at 28 and 32 °C, respectively. Cell cultures were harvested when reaching the mid-exponential growth phase, which was identified by optical density (OD) measurements and their relation to growth functions. Cell suspensions were centrifuged (8 min) at 4000 *g* (Hermle Z300, Hermle Labortechnik, Germany); pellets were washed twice with 0.9% NaCl. For the incubation, we transferred initial cells (grown on LB-medium) as necessary to reach an initial optical density (OD) of 0.1 in the incubation medium.

The incubation medium was a modified ^{2}H-labeled M9 minimal medium, which is commonly used to provide a basic supply of phosphorus, nitrogen, and sulfur.[33] The chemical composition of the medium is described in the Supporting Information (SI). As the only C and energy source, we used 2.5 g L^{-1} of either glucose or lysine (both Campro Scientific, Berlin, Germany). Three stock flasks per C source of the two growth media with varying H isotope ratios were prepared (δ^2H: +150 ‰, +250 ‰ and +500 ‰) by adding the appropriate amounts of sterile 99.99% D_2O (Campro Scientific). For each incubation cycle, 100 mL of the corresponding stock media were filled in 250 mL flasks (Duran, Schott, Mainz, Germany), closed with gas washbottle tops (Duran) and autoclaved.

Incubation. The incubation experiment was carried out for 12 (T1) and 24 h (T2). Two bacterial species, two C sources, three incubation waters with different δ^2H values (δ^2H_{iW}), and two time intervals in triplicates resulted in an experimental setup of 72 incubation flasks. Additionally, an identical setup but without the addition of bacteria was considered as control treatment for the CO_2 production. Cell cultures of both bacteria were incubated at 20 °C. The gas wash bottles were sealed airtight at the top and aerated with C-free synthetic air through a tube on the one side, while the other side was connected with two tubes (Falcon, ThermoFisher, Waltham, MA, USA) filled with NaOH for monitoring CO_2 production. The processing of the samples is described in the SI.

Analyses. *Optical-Density, Flow-Cytometry, CO_2, and Substrate-Concentration Measurements.* All OD measurements to determine the bacterial biomass were performed at 600 nm (Specord 50 Plus, Analytic Jena, Jena, Germany). To guarantee identical initial cell numbers of the two cultures, cell numbers were determined via flow cytometry (Attune Nxt Flow Cytometer, ThermoFisher) and OD was checked before each incubation cycle. Additionally, we calculated bacterial growth (BacG) for each time step as the difference in OD between the final (OD_{ti}) and initial OD (OD_{t0}) according to eq 1:

$$\text{BacG} = \text{OD}_{\text{ti}} - \text{OD}_{\text{to}} \quad (1)$$

For measurements of C mineralization, respired CO_2 was trapped in 1 M NaOH. Detailed information on the calculation of respiration rates is provided in the SI.

Glucose concentrations were determined by the glucose-6-phosphate dehydrogenase-based test kit for glucose (D-glucose UV-test 10 716 251 035. Food Analysis, Boehringer, Mannheim, Germany) using the manufacturer's instructions (https://food.r-biopharm.com/wp-content/uploads/2012/06/roche_ifu_glucose_en_10716251035_2017-11.pdf) and NADPH measurements (Specord 50 Plus, Analytic Jena). Lysine concentrations were measured by HPLC at the Institute of Bio- and Geosciences, Jülich, Germany.

Steam Equilibration and Stable H Isotope Analysis. We used the steam equilibration device based on the design of Wassenaar and Hobson[19] and modified by Ruppenthal et al.[22] to determine $\delta^2H_{n\ bac}$ values of bulk bacterial biomass. Additionally, we measured the total δ^2H values (δ^2H_t) values of glucose ($\delta^2H_{glucose}$ = 91.6 ± 6.3 ‰; n = 6) and lysine (δ^2H_{lysine} = 86.6 ±

https://doi.org/10.1021/acsearthspacechem.2c00085
ACS Earth Space Chem. 2022, 6, 2180−2189

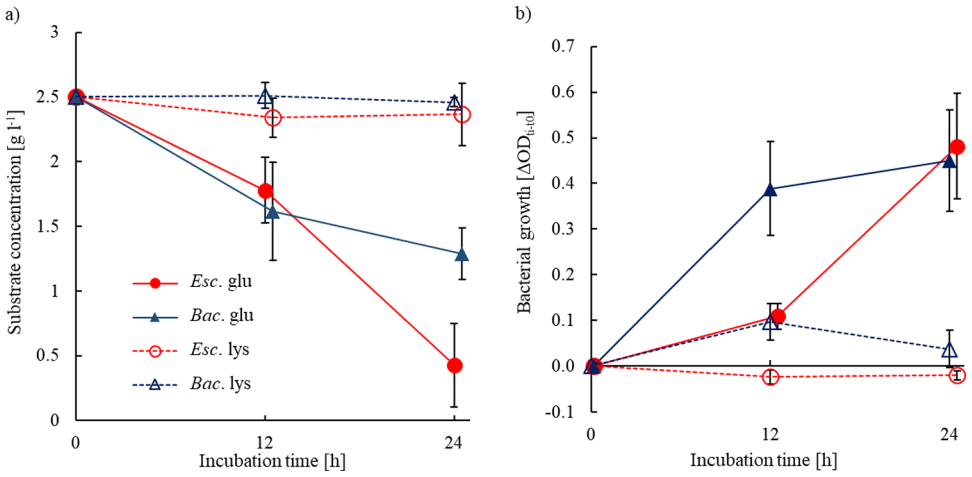

Figure 1. Remaining substrate concentrations in the incubation medium (a) and bacterial growth expressed as the differences in the optical density [OD] at 600 nm between time steps t_i and t_0 ($\Delta OD_{ti\text{-}t0}$) (b) for *B. atrophaeus* (*Bac.*) and *E. coli* (*Esc.*) and the corresponding substrate (glucose (glu) or lysine (lys)) after 12 and 24 h of incubation. Error bars show the standard deviation of substrate concentrations and optical density differences for each time step ($n = 9$). To ease readability, the sampling times have been shifted slightly. Time, substrate, time × bacterial species, and time × substrate significantly ($p < 0.001$) influenced substrate consumption and bacterial growth in the statistical model (Table S1).

4.1 ‰; $n = 6$). Detailed information on the steam equilibration setup, stable H analysis and analytical quality are presented in the SI.

Calculations and Statistical Evaluation. To determine δ^2H values in bacterial biomass, which requires the elimination of the contribution of exchangeable H to δ^2H_t (i) and to quantify the incorporation of ambient-water H into bacterial biomass (ii), we used isotope labeling.[34]

We accounted for the exchangeable O-, N- and S-bonded H in the bacterial species (i) with a mass balance approach adopted from Ruppenthal et al.[6] The total H (H_t) pool consists of an H_{ex} fraction that isotopically exchanges with water vapor and a C-bonded H fraction (H_n) with respective δ^2H_{ex} and δ^2H_n values. Total δ^2H values (δ^2H_t) could be measured directly, and this pool can be described by eq 2.[18,19,35−37]

$$\delta^2H_t = (1 - x_e)\delta^2H_n + x_e\delta^2H_{ex} \quad (2)$$

x_e is the H fraction that is isotopically exchanged during steam equilibration. With regard to different organic compounds, the exchangeable H fraction varies from 0.0 for simple hydrocarbons up to 0.4 (i.e., 40 wt % of H_t) for complex compounds like cellulose, kerogen, or humic acid.[18,19,35,36] If the exchangeable H fraction of a sample is in isotopic equilibrium with the equilibration water, the δ^2H_{ex} value is related to the δ^2H value of the equilibration water (δ^2H_w) with the corresponding equilibrium fractionation factor ($\alpha_{ex\text{-}w}$, eq 3).[6]

$$\alpha_{ex-w} = \frac{\delta^2H_n + 1000}{\delta^2H_{ex} + 1000} \quad (3)$$

The equilibrium fractionation factor $\alpha_{ex\text{-}w}$ depends on the chemical composition of the analyzed samples and the equilibration temperature.[18,19,35,36] However, for chemically complex organic substances, direct experimental determination of $\alpha_{ex\text{-}w}$ is difficult because it would be necessary to assess $\alpha_{ex\text{-}w}$ values through δ^2H values of isotopically equilibrated samples with those of samples with chemically removed H.[19] Recent studies used an approximation of $\alpha_{ex\text{-}w}$ for substances like humic acid, kerogen, keratin, or collagen.[18,19,38] Here, for $\alpha_{ex\text{-}w}$, a provisional value of 1.08 was assigned, which is based on the cellulose equilibrium isotopic fractionation factor between isotopically exchangeable H and water-H for 20 h at 114 °C, which has been experimentally determined.[18] Via a sensitivity analysis over an $\alpha_{ex\text{-}w}$ range of 1.06 to 1.10, Schimmelmann et al.[39] and Wassenaar and Hobson[19] showed that the use of a provisional $\alpha_{ex\text{-}w}$ value is admissible, while the isotopic shift, which is caused by the equilibration procedure, is a function of isotopically exchangeable H and x_e. Therefore, in our study, we used an $\alpha_{ex\text{-}w}$ value of 1.08.

If x_e is constant among aliquots, a plot of δ^2H_t versus δ^2H_w should result in a straight line, defined by eq 4, which is obtained by solving eq 3 for δ^2H_{ex} and substituting into eq 2.[6]

$$\delta^2H_t = x_e\alpha_{ex-w}\delta^2H_w + (1 - x_e)\delta^2H_n + 1000x_e(\alpha_{ex-w} - 1) \quad (4)$$

When all of the isotopically exchangeable H is in equilibrium with the water-H, δ^2H_n from eq 2 is equivalent to δ^2H of the C-bonded H in the sample. Therefore, δ^2H_n can be calculated by rearranging eq 4 to eq 5.[6]

$$\delta^2H_n = \frac{\delta^2H_t - 1000(\alpha_{ex-w} - 1) - x_e\alpha_{ex-w}\delta^2Hw}{(1 - x_e)} \quad (5)$$

For further information about the steam equilibration and the calculation of δ^2H_n values, see Ruppenthal et al.[6]

To trace the incorporation of ambient-water H into the bacterial biomass (ii), we manipulated the H isotope signature of the water during the incubation of bacterial species (δ^2H_{iw}: 150 ‰, 250 ‰, 500 ‰). The incorporation of H from the incubation water will shift the H isotope signature of bacterial species ($\delta^2H_{n\ bac}$ values) toward the δ^2H_{iw} values and result in a straight line (see explanation for eq 4). Therefore, eq 4 can be rewritten as eq 6:

$$\delta^2H_{n\ bac\ ti} = x_{inc}\alpha_{inc-w}\delta^2H_{iw} + (1 - x_{inc})\delta^2H_{n\ bac\ t0} + 1000x_{inc}(\alpha_{inc-w} - 1) \quad (6)$$

with $\delta^2H_{n\ bac\ ti}$ values after incubation composed of a proportion that experienced incorporation ($x_{inc}\alpha_{inc-w}\delta^2H_{iw} + 1000x_{inc}(\alpha_{inc-w} - 1)$) and a proportion that did not ($(1 - x_{inc})\delta^2H_{n\ bac\ t0}$), and $\delta^2H_{n\ bac\ t0}$ reflects the H isotope signature of

https://doi.org/10.1021/acsearthspacechem.2c00085
ACS Earth Space Chem. 2022, 6, 2180−2189

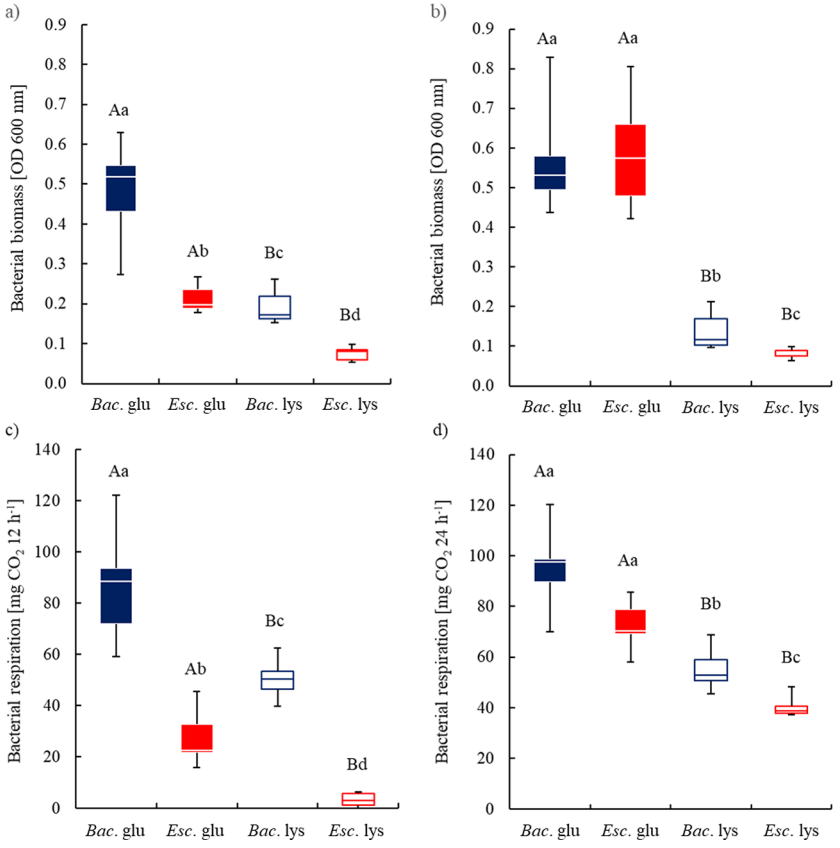

Figure 2. Bacterial biomass (optical density [OD] at 600 nm; (a, b) and bacterial respiration (c, d) of *B. atrophaeus* (*Bac.*) and *E. coli* (*Esc.*) and the corresponding substrate (glucose (glu) or lysine (lys)) after 12 h (a, c) and 24 h (b, d) of incubation. Upper-case letters indicate significant differences between substrates, while lower-case letters show significant differences between the two bacterial species. Error bars show the standard deviation of bacterial biomass and respiration for each treatment (n = 9). Please note that (a) and (b) served as a basis to calculate the difference in the optical density [OD] at 600 nm in Figure 1b.

the bacterial species before incubation. From a mathematical perspective, in the first term, $x_{inc}\alpha_{inc-w}$ represents the slope of the linear regression of $\delta^2H_{n\ bac\ ti}$ on δ^2H_{iw}, while the term $((1 - x_{inc})\delta^2H_{n\ bac\ t0} + 1000x_{inc}(\alpha_{inc-w} - 1))$ represents the y-axis intercept.[6] For the sake of simplicity, Horita and Vass[9] who used a similar approach for two bacterial species assumed no H isotope fractionation associated with the incorporation (α_{inc-w} = 1). However, other studies on bacterial species reported a range of 1.04 to 1.12 for α_{inc-w} associated with incorporation.[20] Therefore, it seems advisable to account for α_{inc-w} in eq 6, which then contains two known variables ($\delta^2H_{n\ bac\ ti}$; $\delta^2H_{n\ bac\ t0}$) and two unknown variables (x_{inc} and α_{inc-w}). We used the Levenberg−Marquardt algorithm as an iterative procedure to estimate the unknown variables.[40,41] As a start value, we used α_{inc-w} = 0.66, which is twice the lowest H isotope fractionation (2 times an ε of −170‰) reported for the production of ^{2}H-depleted photosynthates by autotrophic organisms.[42] For x_{inc}, we set the start value to 0.0001, representing hardly any incorporation. Theoretically, the maximum value for x_{inc} would be 1 (100% incorporation), which was neither exceeded nor reached in our calculations. Linear regressions and estimations of x_{inc} and α_{inc-w} were only calculated in the case of a reliable incorporation, namely, if there were (i) significant differences in $\delta^2H_{n\ bac\ ti}$ values among the three water label treatments and (ii) significantly positive slopes. For all samples in the lysine treatments, the prerequisites were not met. In all cases for which the prerequisites were met, there was a unique solution of the estimates for x_{inc} and α_{inc-w}. In the same way, we calculated x_{inc} and α_{inc-w} based on published linear regressions of δ^2H_{bac} on δ^2H_{iw}.[8,9,20] To extract the exact values of the data points from the published figures, we used the WebPlotDigitizer software (Ankit Rohatgi, Version 4.5, USA). Information on statistical analyses are described in the SI.

RESULTS

Substrate and Species Effects on Bacterial Performance. The interpretation of the ^{2}H incorporation requires the understanding of the bacterial performance during the incubation experiment. Therefore, we assessed a number of vital properties of the two studied bacterial species. Despite the hardly detectable lysine consumption, *B. atrophaeus* did show a small growth rate (Figure 1; means significantly different from zero, $p \leq 0.03$). By contrast, we observed a die-off of a proportion of *E. coli* in the lysine treatment (Figure 1; bacterial growth negative and significantly different from zero; $p \leq 0.003$). In the glucose treatment, *E. coli* consumed more substrate than *B. atrophaeus*, yet this difference was significant after 24 h only (Figure 1a; significant time × bacterial species interaction in Table S1). In line, from 12 to 24 h, the growth increase of *E. coli* was larger than that of *B. atrophaeus* in the glucose treatment (Figure 1b; significant time × bacterial species interaction in Table S1).

The ^{2}H concentration in the used incubation waters had no effect on the bacterial consumption of lysine or glucose, the bacterial growth (BacG), and the respiration ($p > 0.25$, Table S1). Lysine concentrations hardly changed with time in the

https://doi.org/10.1021/acsearthspacechem.2c00085
ACS Earth Space Chem. 2022, 6, 2180−2189

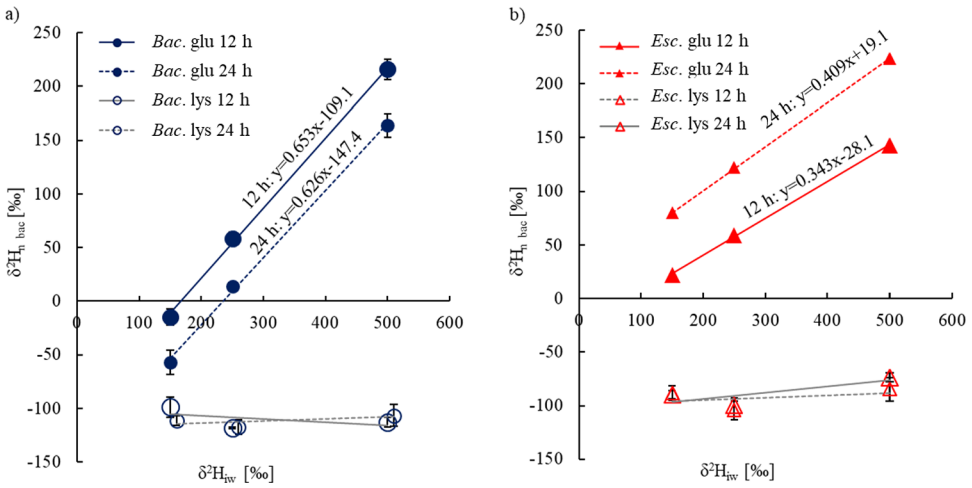

Figure 3. Regression of the $\delta^2H_{n\ bac}$ values of *B. atrophaeus* (*Bac.*) (a) and *E. coli* (*Esc.*) (b) on the δ^2H_{iw} values (+150, +250, +500 ‰) for glucose (glu) or lysine (lys) after 12 (solid lines) and 24 h (dashed lines) of incubation. If the regression line of $\delta^2H_{n\ bac}$ values on δ^2H_{iW} values did not significantly differ from zero indicating that ^{2}H-enriched water labels did not result in more positive $\delta^2H_{n\ bac}$ values, lines were colored in gray and the regression equation was excluded. Error bars show the standard deviation of $\delta^2H_{n\ bac}$ values for each time step (n = 3).

Table 1. Compilation of the Results for Bacterial Species, Analyzed Compartment, Culture Medium with the Means of Calculated Incorporation (x_{inc}), and the Isotope Fractionation (Expressed Both as $\alpha_{inc\text{-}w}$ and $\varepsilon_{BacBiom/w}$) of our Incubation Experiment and Recalculated Values for Data of Previously Published Studies According to Eqs 6 and 7

source	bacterial species	compartment	culture medium	time [h]	x_{inc} [%]	$\alpha_{inc\text{-}w}$	$\varepsilon_{BacBiom/w}$ [‰]
this study	*B. atrophaeus*	cells	M9 minimal medium (MM) + glucose	12	78.2 ± 6.0	0.835 ± 0.001	−165 ± 1
			M9 MM + glucose	24	79.4 ± 5.7	0.789 ± 0.004	−207 ± 6
	E. coli	cells	M9 MM + glucose	12	42.4 ± 2.7	0.809 ± 0.004	−191 ± 4
			M9 MM + Glucose	24	44.1 ± 3.1	0.927 ± 0.000	−72 ± 1
Kreuzer-Martin et al.[20]	*B. subtilis*	cells	Schaeffer's sporulation medium (SSM)	3	10.9	1.171	171
		spores	SSM	48	35.6	0.785	−215
Kreuzer-Martin et al.[8]	*B. subtilis*	spores	Difco SSM	48	26.9	1.041	41
		spores	Oxoid SSM	48	34.8	0.832	−168
		spores	Luria-Bertani	48	33.0	0.970	−30
		spores	Difco SSM + Glucose	48	30.3	1.022	22
		spores	Oxoid SSM + Glucose	48	33.1	0.996	−4
Horita and Vass[9]	*B. subtilis*	cells	BBL Trypticase Soy Broth -TSB (Soybean-Casein Digest Medium)	96	26.3	0.974	−26
	E. agglomerans	cells	BBL Trypticase Soy Broth -TSB	96	35.7	0.790	−210

incubations with both test organisms (*B. atrophaeus* and *E. coli*; Figure 1a and Table S1). In contrast, glucose concentrations decreased significantly with time in the incubations with both test organisms (Figure 1a and Table S1). The glucose consumption was reflected in increased total bacterial biomass production, growth, and respiration in the glucose than in the lysine treatments (Figures 1b and 2a,b and Table S1). On average, the total bacterial biomass production on glucose was 273% higher than on lysine. In general, the effect of substrate on bacterial performance was more pronounced after 24 h (Figures 1 and 2 and Table S1) with the exception of respiration for which the substrate effect was similar between the sampling periods (non-significant time × substrate interactions in Table S1). Accordingly, respiration standardized to the bacterial biomass was significantly higher particularly after 24 h in the lysine treatments (*B. atrophaeus*: 4.3 ± standard deviation of 1.4 mg CO_2 $(10^3$ cells$)^{-1}$; *E. coli*: 1.0 ± 0.24 mg CO_2 $(10^3$ cells$)^{-1}$) as compared to the glucose treatments (0.9 ± 0.8 mg CO_2 $(10^3$ cells$)^{-1}$; Table S2). The substrate effects were consistent for both bacterial species (Figures 1 and 2; non-significant bacterial species × substrate interactions in Table S2).

Biomass production and respiration of *B. atrophaeus* were larger than those of *E. coli* particularly after 12 h (Figure 2; Table S1). After 24 h, we did not observe a significant difference in the total respiration between bacterial species for glucose anymore (Table S1, mean of 83.4 ± 15.9 mg CO_2). For lysine, this effect was still pronounced (55.6 ± 6.8 mg CO_2 (*B. atrophaeus*) and 40.1 ± 3.4 mg CO_2 (*E. coli*); Figure 2c,d; significant time × bacterial species interaction in Table S1). The same was true when respiration was standardized to bacterial biomass. There was a significant difference in respiration between bacterial species in the glucose treatment after 24 h ($p < 0.001$; *B. atrophaeus*: 1.7 ± 0.4 mg CO_2 $(10^3$ cells$)^{-1}$, *E. coli*: 0.26 mg ± 0.04 mg CO_2 $(10^3$ cells$)^{-1}$; Table S2).

Substrate and Species Effects on δ^2H_n Values of Bacteria and H Incorporation. Initial pre-cultures of *B. atrophaeus* grown on LB-medium tended to show of lower exchangeable H concentrations (19.1%; n = 2) compared with *E.*

https://doi.org/10.1021/acsearthspacechem.2c00085
ACS Earth Space Chem. 2022, 6, 2180−2189

coli (25.3%; $n = 2$). After incubation in the M9 minimal medium with either glucose or lysine, *B. atrophaeus* had a significantly larger contribution of exchangeable H (23.4 ± 6.0%) than *E. coli* (19.4 ± 3.4%; Tables S1 and S3).

The δ^2H_n values of the inocula of the bacterial species ranged between −119.8 and −115.7 ‰ (*B. atrophaeus* for the 12 and 24 h incubations, respectively; $n = 1$ for each incubation duration) and between −163.0 and −168.8 ‰ (*E. coli* for the 12 and 24 h incubations, respectively). We did not evaluate the effects of time and bacterial species on δ^2H_n values of the bacterial species ($\delta^2H_{n\ bac}$) during the incubation. Nevertheless, the effect of water can be assessed independently and this was different for the substrates (significant substrate × water interaction in Table S1).

$\delta^2H_{n\ bac}$ values in the lysine treatment did not increase with increasingly ^{2}H-enriched incubation waters for each bacterial species (mean and standard deviations of the $\delta^2H_{n\ bac}$ values for both incubation times: *B. atrophaeus*: −110.8 ± 9.4 ‰, *E. coli*: −90.2 ± 12.4 ‰; Figure 3). Accordingly, the slope of the regression of $\delta^2H_{n\ bac}$ values on δ^2H_{iw} values did not differ significantly from zero ($0.49 > p > 0.07$) and no incorporation from ambient-water H was detected for the lysine treatment (therefore not included in Table S1). Nevertheless, the $\delta^2H_{n\ bac}$ values during the incubation were enriched in ^{2}H as compared to initial $\delta^2H_{n\ bac}$ values ($\varepsilon_{ti/t0}$; *B. atrophaeus*: 7.9 ± 10.7 ‰; *E. coli*: 90.8 ± 14.6 ‰) and this difference significantly differed from zero ($p \leq 0.007$; Figure 3).

In contrast to the lysine treatment, $\delta^2H_{n\ bac}$ values in the glucose treatment differed significantly among the three ^{2}H-enriched incubation water treatments for both bacterial species (Figure 3 and Table S1). Based on the regression, we estimated the incorporation of ambient-water H into the C-bonded H in bacterial biomass (x_{inc}) and the associated isotope fractionation ($\alpha_{inc\text{-}w}$, $\varepsilon_{BacBiom/w}$; Table 1). x_{inc} did not change with time and was consistently larger for *B. atrophaeus* (mean of the two incubation periods 79.0 ± 5.9%) than for *E. coli* (43.2 ± 3.0%; Table S1). The associated isotope fractionation was also different for the two bacterial species (Table S1). However, the species-specific effect changed with time (Table S1) and was related to the growth rates: if growth rates were small (after 12 h for *E. coli* and after 24 h for *B. atrophaeus*), $\varepsilon_{BacBiom/w}$ was comparable between species, while it differed between species if growth rates were large (after 12 h for *B. atrophaeus* and after 24 h for *E. coli*).

DISCUSSION

H Incorporation into C-Bonded H in the Glucose Treatment. In the glucose treatment, substrate consumption, bacterial growth, bacterial biomass, and respiration were significantly higher than in the lysine treatment (Figures 1 and 2). This is in line with the first part of hypothesis (i) and with positive effects of glucose on bacterial growth,[43,44] bacterial biomass,[45] and bacterial respiration.[46,47] Growth involves endergonic, anabolic reactions during biosynthesis that are enabled by energy transfer by adenosine triphosphate (ATP).[48] The glycolysis pathway requires glucose as the reaction educt,[49] and glucose degradation generates ATP because the net balance is the gain of two ATP molecules per molecule of glucose.[50] This positive net balance of ATP allows bacteria to build up cell compounds and thus can explain the positive effect of glucose on bacterial performance.

Along with the positive effect of glucose on bacterial performance, we found substantial incorporation (39 to 86%) of ambient-water H into the C-bonded H pool of bacteria in the glucose treatment (Table 1). This also supports the first part of hypothesis (i) and is higher than the incorporation of ambient-water H in previous bacterial studies ranging from 11 to 36% (Table 1). In these previous studies, a re-equilibration of H_{ex} with vapor in ambient air after incubation and before H isotope measurements cannot be excluded but could hinder the detection of ^{2}H-enriched H and might have reduced the labeling efficiency. Therefore, incorporation of ambient-water H is underestimated if the exchangeable H is included.[8,9,17,20,21] In line with our results on the nonexchangeable, C-bonded H fraction, 70% of H in lipids was derived from ambient-water H during decomposition of soil organic matter and this incorporation was mostly driven by bacterial biosynthesis.[51] As opposed to the situation described below for the lysine treatment, ^{2}H from ambient water was incorporated into C-bonded H during glycolysis and the resulting compounds were not oxidized completely but were retained in organismic tissue. This retention is possible via the anabolic mode of the TCA cycle. In anabolic processes, intermediates of the TCA are used for the synthesis of various compounds. For example, acetyl coenzyme A (CoA), which is generated, e.g., from the pyruvate produced by the glycolysis pathway, is an important building block of metabolic intermediates in the central C metabolism[52] and a precursor of many anabolic reactions.[53] The fact that the incorporation of ambient-water H into C-bonded H did not change over time (Table 1) indicates that catabolic reactions (= loss of incorporated ^{2}H) and anabolic reactions (= preservation of incorporation of ^{2}H) keep pace with each other if glucose is available as a substrate.

In contrast to the last part of hypothesis (i), we found that the incorporation of ambient-water H significantly differed between the two bacterial species (Figure 3; Table 1). This species-specific difference was constant with time (Table S1), although the species effect on bacterial performance was not (Figures 1 and 2). For example, *E. coli* grew and respired less than *B. atrophaeus* after 12 h, whereas growth and respiration of the two species did not differ after 24 h. Therefore, not the metabolism but the species seem to be relevant for the extent of incorporation of ambient-water H into bacterial biomass. Such species-specific differences in the extent of incorporation of ambient-water H might be related to different contributions of biosynthesis pathways and thus ultimately to a species-specific chemical composition of bacterial biomass. For example, Gram-positive and Gram-negative bacteria differ in terms of the composition of the cell wall.[54] Peptidoglycan (PG) is the building block of cell walls composed of units of *N*-acetyl-glucosamine-*N*-acetyl-muramic acid cross-linked via pentapeptide chains.[55] Cells and spores of Gram-positive bacteria such as *B. atrophaeus* are surrounded by a thick PG layer that accounts for up to 90% of the bacterial dry weight.[56] By contrast, the PG layer contributes only 10% in Gram-negative bacteria such as *E. coli*.[56] *N*-Acetyl-glucosamine is a derivative of glucose, and *N*-acetyl-muramic acid is a glucose molecule with an acetylated amid at the C_2 position.[57,58] Their synthesis structurally binds acetyl-CoA. Therefore, a thicker layer of PG in *B. atrophaeus* would also reflect a higher glycolysis-related incorporation of ambient-water H than in *E. coli*, which is in line with our results. This reasoning is also corroborated by a larger proportion of H_{ex} in *B. atrophaeus* than in *E. coli* (Table S3) because of an increased contribution of O- and N-bonded H in hydroxyl, carboxyl, and amine groups in the PG layer. In summary, the pronounced effect of glucose corroborates glycolysis as the mechanism underlying the incorporation of ambient-water H into

https://doi.org/10.1021/acsearthspacechem.2c00085
ACS Earth Space Chem. 2022, 6, 2180−2189

organismic tissue. However, the subsequent biosynthesis pathways likely determine the extent of incorporation into micorbial biomass, which is species-specific.

H Incorporation into C-Bonded H in the Lysine Treatment. *E. coli* showed a partial die-off, while *B. atrophaeus* maintained growth, yet at slow rates, if lysine was provided as a substrate (Figure 1). Irrespective of bacterial growth, both bacterial species maintained metabolism as indicated by respiration (Figure 2b), which is contrary to our expectation (first part of hypothesis (ii)). In the case of C starvation of *E. coli*, lysine could be recycled in the stationary phase (cease of growth while metabolism continues) and catabolic reactions[25] that oxidize organic compounds to CO_2, e.g., in the TCA cycle, promote the energy regeneration. Knorr et al.[25] demonstrated the catabolic degradation during the central metabolic pathway of lysine to succinate in *E. coli* via intermediates of glutarate and L-2-hydroxyglutarate in wildtype *E. coli*. Compared with Knorr et al.,[25] our incubation was not conducted under optimal conditions. More importantly, our M9 minimal medium was not supplemented with glucose as a C and energy source. The results of Knorr et al.[25] suggest that the bacteria need a readily available C source to metabolize lysine. The addition of glucose therefore ensured basic glycolytic activity, which could explain that *E. coli* was not able to show bacterial growth in our experiment with lysine as the sole C source.

Because *B. atrophaeus* is not able to use lysine as an energy source but also continued metabolic activity, a more likely explanation for the observed ongoing bacterial respiration without substrate consumption might be the bacterial consumption of dead cells. During starvation, cell membranes lose integrity[59] and *E. coli* recycles metabolites from dead cells, which sustains the viability of the remaining culture.[60] For *Bacillus subtilis*, González-Pastor et al.[61] described that cells that entered the sporulation pathway act cooperatively by blocking sister cells to sporulate, causing the latter to lyse, which allows others to keep on metabolizing, and consequently, its siblings are cannibalized. In line, we found an indication of sporulation for the extracted bacterial pellets of *B. atrophaeus*, which showed a red color.[62] Therefore, in contrast to hypothesis (ii), not the metabolic pathways but the bacterial recycling decided about the bacterial performance of *E. coli* and *B. atrophaeus* in the lysine treatment.

The lack of an incorporation of ambient-water H in the lysine treatment (Figure 3) in principle corroborates the second part of hypothesis (ii). However, this could have been simply attributable to the lacking lysine consumption and growth (Figure 1). Therefore, we cannot confirm that incorporation of ambient-water H does not take place without glycolysis because this would have required an uptake of lysine by the bacterial species, which was not the case. Nevertheless, the lack of incorporation of ambient-water H in the lysine treatment is different from studies showing such an incorporation for any metabolically active bacteria.[8,9,17,20,21] Irrespective of the C source, the measured respiration rates suggest that the studied bacteria were metabolically active. The stressful conditions indicated by large respiration:cell number ratios[46,63,64] in the lysine treatment were more pronounced for *B. atrophaeus* than *E. coli* at both sampling times and even only showed up for *E. coli* after 24 h of incubation (Figure S1). This stress likely forced the bacterial species to produce energy for basic metabolism in the absence of a suitable growth substrate. Yet, despite basic metabolic activity, we could not calculate H incorporation for the lysine treatment. Knowledge on reaction pathways of metabolic activity under sub-optimal growth conditions is scarce.[60,65] Nevertheless, although glycolysis as part of the basic metabolism might have involved the incorporation of ^2H from the isotopically labeled incubation waters in our study, the C−^2H bond in GAP can be broken again during subsequent oxidation steps in the TCA cycle. We speculate that a respiration-driven ^2H incorporation was no longer detectable because the former synthesized C−^2H bonds were completely oxidized to CO_2. In other words, the amphibolic TCA cycle worked in the catabolic mode that serves to generate energy. In summary, the incorporation of ambient-water H into the C-bonded H fraction was negligible in the studied bacteria under the specific stressful conditions of our lysine treatment.

Strikingly, although the complete conversion to CO_2 should have eradicated any isotope effect, a significant, label-independent ^2H enrichment of $\delta^2H_{n\ bac}$ values after incubation as compared to initial $\delta^2H_{n\ bac}$ values for bacterial species was observed in the lysine treatment ($\varepsilon_{ti/t0}$; *B. atrophaeus*: 7.9 ± 10.7 ‰; *E. coli*: 90.8 ± 14.6 ‰). In general, a ^2H enrichment in bacteria growing on substrates involved in the TCA cycle was also reported for lipids[26,29] although the ^2H enrichment was less pronounced under stationary phase conditions.[29] The ^2H enrichment was attributed to positive isotope fractionation factors associated with the reduction of nicotinamide adenine dinucleotide phosphate ($NADP^+$) by dehydrogenase and transhydrogenase enzymes.[29,66] Because these reactions involve hydride transfers also from ambient water,[15,26] which we did not find, NADPH-related reactions cannot explain the ^2H enrichment of bacteria in our incubation. Alternatively, kinetic isotope fractionation associated with the complete conversion of R−C−^2H to H_2O and CO_2 might result in a ^2H enrichment in the remaining bacterial biomass and a ^2H depletion in the produced H_2O. Similarly, during SOM decomposition, ^{13}C enrichment in the remaining SOM and ^{13}C depletion in the produced CO_2 were reported.[67,68] Furthermore, a ^2H depletion in intracellular water due to metabolic activity of *E. coli* was also reported by Kreuzer-Martin et al.[69] Notably, the ^2H depletion was most pronounced under stressful (stationary phase) conditions[69] that also apply to our lysine treatment. In summary, the type of growth substrate and the resulting importance of catabolic reactions dictate whether the incorporation of ambient-water H will leave an imprint on the bacterial species.

Isotope Fractionation Associated with H Incorporation into C-Bonded H. In the case of relatively small growth rates (*E. coli* after 12 h; *B. atrophaeus* after 24 h; Figure 1b), $\varepsilon_{BacBiom/w}$ was around −200 ‰ for both species (Table 1). This is in line with hypothesis (iii). However, during pronounced growth (*E. coli* after 24 h; *B. atrophaeus* after 12 h; Figure 1b), $\varepsilon_{BacBiom/w}$ was less negative and differed between the two studied bacteria species (Table S1). This is contrary to our expectation and to the postulation of species-independent H isotope fractionation factors.[26] Furthermore, several studies suggested that heterotrophic metabolism results in an enrichment in ^2H in the synthesized product relative to ambient water,[7,15,29] which is the opposite of what we found. Nevertheless, other studies confirm that $\varepsilon_{BacBiom/w}$ can be as low as −215 ‰[20] (Table 1). In conjunction with our findings related to the importance of reactions involved in metabolism (Section 4.1), we propose that the highly variable $\varepsilon_{BacBiom/w}$ values are a result of different growth-induced net apparent fractionation factors. In agreement, different H isotope fractionations during lipid synthesis in bacteria in stationary and exponential growth phases were reported.[29] In more detail, Wijker et al.[26] argued that not only

https://doi.org/10.1021/acsearthspacechem.2c00085
ACS Earth Space Chem. 2022, 6, 2180−2189

^{2}H enrichment but also ^{2}H depletion is possible in bacterial lipids. They found ^{2}H depleted lipids in *E. coli* and attributed this to an imbalance between the demand for NADPH as reducing agent for anabolic reactions and catabolic NADPH production.[26] The NADPH underproduction shifts the net apparent isotope fractionation from ^{2}H enrichment in NADPH as a reaction product toward ^{2}H depletion in NADH as the reaction educt.[26] Such an imbalanced NADPH consumption and production was not only evident in *E. coli* but also in *B. subtilis*.[26] Consequently, our results suggest a species-independent H isotope fractionation. However, we cannot tease apart the effect of growth rates and metabolic fluxes from species because the two species varied in growth (Figure 1b) and metabolic rates. In summary, growth conditions and likely the related metabolic fluxes influence the isotope fractionation associated with the incorporation of ambient-water H into bacterial biomass.

Our results show that bacteria adjust δ^2H_n values to the H isotopic composition of ambient water during metabolism, and therefore, δ^2H_n values of bacteria are not isotopically stable. On the one hand, the influence of metabolic flux rates under changing environmental conditions constrains the assignment of bacterial origins and thus of soil samples based on H isotope ratios. However, under stressful conditions, the isotopic composition of water is not incorporated into bacterial biomass because bacteria switch to catabolic metabolism. Stressful conditions imply, e.g., desiccation,[70] nutrient limitation,[71] and starvation,[72] especially starvation of glucose,[73,74] leading to increased catabolic activity. Under these conditions, soil samples will preserve the imprint of ambient water on δ^2H_n values of SOM at the sample location. On the other hand, the H isotope approach opens up new opportunities to study growth conditions of bacteria under different environmental conditions together with different bacterial activities and metabolism. Furthermore, our results improve the understanding of microbial modification of δ^2H_n values in soil organic matter (SOM) and might moreover be useful to assess the microbial input to SOM.

■ ASSOCIATED CONTENT

Supporting Information

The Supporting Information is available free of charge at https://pubs.acs.org/doi/10.1021/acsearthspacechem.2c00085.

> Material and methods including medium preparation, sample processing, calculation of respiration, details of the steam equilibration setup, stable H analysis, and quality specifications, statistical analyses and results with CO_2-production per 10^3 cells (Figure S1), and results of the statistical evaluation (Tables S1 and S2) (PDF)

■ AUTHOR INFORMATION

Corresponding Author

Yvonne Oelmann − *Geoecology, University of Tübingen, 72070 Tübingen, Germany;* orcid.org/0000-0003-3513-6568; Email: yvonne.oelmann@uni-tuebingen.de

Authors

Arnim Kessler − *Geoecology, University of Tübingen, 72070 Tübingen, Germany*

Stefan Merseburger − *Institute of Geography and Geoecology, Karlsruhe Institute of Technology (KIT), 76131 Karlsruhe, Germany*

Andreas Kappler − *Geomicrobiology, University of Tübingen, 72076 Tübingen, Germany;* orcid.org/0000-0002-3558-9500

Wolfgang Wilcke − *Institute of Geography and Geoecology, Karlsruhe Institute of Technology (KIT), 76131 Karlsruhe, Germany;* orcid.org/0000-0002-6031-4613

Complete contact information is available at: https://pubs.acs.org/10.1021/acsearthspacechem.2c00085

Notes

The authors declare no competing financial interest.

■ ACKNOWLEDGMENTS

We thank Lars Grimm, Ellen Röhm, and Dr. Casey Bryce for the technical support in the microbiology laboratory and Sabine Flaiz for advice and assistance in EA-IRMS analyses. We also thank Prof. Dr. Jan Marienhagen and Sascha Sokolowsky (Institute of Bio- and Geosciences; Jülich) for lysine analysis. The study was funded by the German Research Foundation (DFG, OE516/11-1).

■ REFERENCES

(1) Meier-Augenstein, W.; Hobson, K. A.; Wassenaar, L. I. Critique: measuring hydrogen stable isotope abundance of proteins to infer origins of wildlife, food and people. *Bioanalysis* **2013**, *5*, 751−767.

(2) Hallworth, M. T.; Marra, P. P.; McFarland, K. P.; Zahendra, S.; Studds, C. E. Tracking dragons: stable isotopes reveal the annual cycle of a long-distance migratory insect. *Biol. Lett.* **2018**, *14*, 20180741.

(3) Hobson, K. A.; Doward, K.; Kardynal, K. J.; Mcneil, J. N. Inferring origins of migrating insects using isoscapes: a case study using the true armyworm, *Mythimna unipuncta*, in North America. *Ecol. Entomol.* **2018**, *43*, 332−341.

(4) Bowen, G. J.; Wassenaar, L. I.; Hobson, K. A. Global application of stable hydrogen and oxygen isotopes to wildlife forensics. *Oecologia* **2005**, *143*, 337−348.

(5) West, J. B.; Bowen, G. J.; Dawson, T. E.; Tu, K. P. *Isoscapes*. Springer Netherlands: Dordrecht, 2010, DOI: 10.1007/978-90-481-3354-3.

(6) Ruppenthal, M.; Oelmann, Y.; Wilcke, W. Isotope ratios of nonexchangeable hydrogen in soils from different climate zones. *Geoderma* **2010**, *155*, 231−241.

(7) Ruppenthal, M.; Oelmann, Y.; del Valle, H. F.; Wilcke, W. Stable isotope ratios of nonexchangeable hydrogen in organic matter of soils and plants along a 2100-km climosequence in Argentina: New insights into soil organic matter sources and transformations? *Geochim. Cosmochim. Acta* **2015**, *152*, 54−71.

(8) Kreuzer-Martin, H. W.; Chesson, L. A.; Lott, M. J.; Dorigan, J. V.; Ehleringer, J. R. Stable isotope ratios as a tool in microbial forensics—Part 1. Microbial isotopic composition as a function of growth medium. *J. Forensic Sci.* **2004**, *49*, 1−7.

(9) Horita, J.; Vass, A. A. Stable-isotope fingerprints of biological agents as forensic tools. *J. Forensic Sci.* **2003**, *48*, 2002170.

(10) Berg, J. M.; Tymoczko, J. L.; Stryer, L. *Biochemistry* 7th ed., Freeman Palgrave Macmillan: New York, NY 2012.

(11) Gerlt, J. A. Stabilization of Reactive Intermediates and Transition States in Enzyme Active Sites by Hydrogen Bonding. In: *Comprehensive Natural Products Chemistry*; 5−29. Elsevier, 1999.

(12) Knowles, J. R.; Albery, W. J. Perfection in enzyme catalysis: the energetics of triosephosphate isomerase. *Acc. Chem. Res.* **1977**, *10*, 105−111.

(13) Rieder, S. V.; Rose, I. A. The mechanism of the triosephosphate isomerase reaction. *J. Biol. Chem.* **1959**, *234*, 1007−1010.

(14) Whitman, C. P. Keto−Enol Tautomerism in Enzymatic Reactions. In: *Comprehensive Natural Products Chemistry*; 31−50. Elsevier, 1999.
(15) Yakir, D. Variations in the natural abundance of oxygen-18 and deuterium in plant carbohydrates. *Plant, Cell Environ.* **1992**, *15*, 1005−1020.
(16) Bren, A.; Park, J. O.; Towbin, B. D.; Dekel, E.; Rabinowitz, J. D.; Alon, U. Glucose becomes one of the worst carbon sources for *E. coli* on poor nitrogen sources due to suboptimal levels of cAMP. *Sci. Rep.* **2016**, *6*, 24834.
(17) Fogel, M. L.; Griffin, P. L.; Newsome, S. D. Hydrogen isotopes in individual amino acids reflect differentiated pools of hydrogen from food and water in *Escherichia coli*. *Proc. Natl. Acad. Sci. U. S. A.* **2016**, *113*, E4648−E4653.
(18) Schimmelmann, A. Determination of the concentration and stable isotopic composition of nonexchangeable hydrogen in organic matter. *Anal. Chem.* **1991**, *63*, 2456−2459.
(19) Wassenaar, L. I.; Hobson, K. A. Improved method for determining the stable-hydrogen isotopic composition (δD) of complex organic materials of environmental interest. *Environ. Sci. Technol.* **2000**, *34*, 2354−2360.
(20) Kreuzer-Martin, H. W.; Lott, M. J.; Dorigan, J.; Ehleringer, J. R. Microbe forensics: oxygen and hydrogen stable isotope ratios in Bacillus subtilis cells and spores. *Proc. Natl. Acad. Sci. U. S. A.* **2003**, *100*, 815−819.
(21) Kreuzer-Martin, H. W.; Jarman, K. H. Stable isotope ratios and forensic analysis of microorganisms. *Appl. Environ. Microbiol.* **2007**, *73*, 3896−3908.
(22) Ruppenthal, M.; Oelmann, Y.; Wilcke, W. Optimized demineralization technique for the measurement of stable isotope ratios of nonexchangeable H in soil organic matter. *Environ. Sci. Technol.* **2013**, *47*, 949−957.
(23) Neshich, I. A. P.; Kiyota, E.; Arruda, P. Genome-wide analysis of lysine catabolism in bacteria reveals new connections with osmotic stress resistance. *ISME J.* **2013**, *7*, 2400−2410.
(24) Newsholme, P.; Stenson, L.; Sulvucci, M.; Sumayao, R.; Krause, M. Amino Acid Metabolism. In: *Comprehensive Biotechnology*; 3−14. Elsevier, 2011.
(25) Knorr, S.; Sinn, M.; Galetskiy, D.; Williams, R. M.; Wang, C.; Müller, N.; Mayans, O.; Schleheck, D.; Hartig, J. S. Widespread bacterial lysine degradation proceeding via glutarate and L-2-hydroxyglutarate. *Nat. Commun.* **2018**, *9*, 5071.
(26) Wijker, R. S.; Sessions, A. L.; Fuhrer, T.; Phan, M. 2H/1H variation in microbial lipids is controlled by NADPH metabolism. *Proc. Natl. Acad. Sci. U. S. A.* **2019**, *116*, 12173−12182.
(27) Jackson, J. B.; Peake, S. J.; White, S. A. Structure and mechanism of proton-translocating transhydrogenase. *FEBS Lett.* **1999**, *464*, 1−8.
(28) O'Leary, M. H. Multiple isotope effects on enzyme-catalyzed reactions. *Annu. Rev. Biochem.* **1989**, *58*, 377−401.
(29) Heinzelmann, S. M.; Villanueva, L.; Sinke-Schoen, D.; Sinninghe Damsté, J. S.; Schouten, S.; van der Meer, M. T. J. Impact of metabolism and growth phase on the hydrogen isotopic composition of microbial fatty acids. *Front. Microbiol.* **2015**, *6*, 408.
(30) Zhao, W.; Fang, J.; Huang, X.; Zhang, Y.; Liu, W.; Wang, Y.; Zhang, L. Carbon and hydrogen isotope fractionation in lipid biosynthesis by *Sporosarcina* sp. DSK25. *Geochem. Perspect. Lett.* **2020**, 9−13.
(31) Sessions, A. L.; Burgoyne, T. W.; Schimmelmann, A.; Hayes, J. M. Fractionation of hydrogen isotopes in lipid biosynthesis. *Org. Geochem.* **1999**, *30*, 1193−1200.
(32) Fang, J.; Li, C.; Zhang, L.; Davis, T.; Kato, C.; Bartlett, D. H. Hydrogen isotope fractionation in lipid biosynthesis by the piezophilic bacterium *Moritella japonica* DSK1. *Chem. Geol.* **2014**, *367*, 34−38.
(33) Xiao, J.; Elf, J..; Li, G.; Ji, Y.; Xie, G. S. Imaging Gene Expression in Living Cells at the Single-Molecule Level. In: *Single Molecules: A Laboratory Manual*; Selvin, P.; Ha, T., Eds.; Cold Spring Harbor Laboratory Press: Cold Spring Harbor, NY 2007. 2008.
(34) Kessler, A.; Kreis, K.; Merseburger, S.; Wilcke, W.; Oelmann, Y. Incorporation of hydrogen from ambient water into the C-bonded H pool during litter decomposition. *Soil Biol. Biochem.* **2021**, *162*, No. 108407.
(35) Feng, X.; Krishnamurthy, R. V.; Epstein, S. Determination of ratios of nonexchangeable hydrogen in cellulose: A method based on the cellulose-water exchange reaction. *Geochim. Cosmochim. Acta* **1993**, *57*, 4249−4256.
(36) Filot, M. S.; Leuenberger, M.; Pazdur, A.; Boettger, T. Rapid online equilibration method to determine the D/H ratios of non-exchangeable hydrogen in cellulose. *Rapid Commun. Mass Spectrom.: RCM* **2006**, *20*, 3337−3344.
(37) Sessions, A. L.; Hayes, J. M. Calculation of hydrogen isotopic fractionations in biogeochemical systems. *Geochim. Cosmochim. Acta* **2005**, *69*, 593−597.
(38) Sauer, P. E.; Schimmelmann, A.; Sessions, A. L.; Topalov, K. Simplified batch equilibration for D/H determination of non-exchangeable hydrogen in solid organic material. *Rapid Commun. Mass Spectrom.: RCM* **2009**, *23*, 949−956.
(39) Schimmelmann, A.; Lewan, M. D.; Wintsch, R. P. D/H isotope ratios of kerogen, bitumen, oil, and water in hydrous pyrolysis of source rocks containing kerogen types I, II, IIS, and III. *Geochim. Cosmochim. Acta* **1999**, *63*, 3751−3766.
(40) Levenberg, K. A method for the solution of certain non-linear problems in least squares. *Quart. Appl. Math.* **1944**, *2*, 164−168.
(41) Marquardt, D. W. An Algorithm for Least-Squares Estimation of Nonlinear Parameters. *J. Soc. Ind. Appl. Math.* **1963**, *11*, 431−441.
(42) Yakir, D.; Deniro, M. J. Oxygen and hydrogen isotope fractionation during cellulose metabolism in *Lemna gibba* L. *Plant Physiol.* **1990**, *93*, 325−332.
(43) Blagodatskaya, E.; Kuzyakov, Y. Active microorganisms in soil: Critical review of estimation criteria and approaches. *Soil Biol. Biochem.* **2013**, *67*, 192−211.
(44) Mau, R. L.; Liu, C. M.; Aziz, M.; Schwartz, E.; Dijkstra, P.; Marks, J. C.; Price, L. B.; Keim, P.; Hungate, B. A. Linking soil bacterial biodiversity and soil carbon stability. *ISME J.* **2015**, *9*, 1477−1480.
(45) Sparling, G. P. Microcalorimetry and other methods to assess biomass and activity in soil. *Soil Biol. Biochem.* **1981**, *13*, 93−98.
(46) Anderson, T.-H.; Domsch, K. H. Soil microbial biomass: The eco-physiological approach. *Soil Biol. Biochem.* **2010**, *42*, 2039−2043.
(47) Ehlers, K.; Bakken, L. R.; Frostegård, Å.; Frossard, E.; Bünemann, E. K. Phosphorus limitation in a Ferralsol: Impact on microbial activity and cell internal P pools. *Soil Biol. Biochem.* **2010**, *42*, 558−566.
(48) Repke, K. R. H. Reinstatement of the ATP high energy paradigm. *Mol. Cell. Biochem.* **1996**, *160-161*, 95−99.
(49) Zhang, S.; Yang, W.; Chen, H.; Liu, B.; Lin, B.; Tao, Y. Metabolic engineering for efficient supply of acetyl-CoA from different carbon sources in *Escherichia coli*. *Microb. Cell Fact.* **2019**, *18*, 130.
(50) Chaudhry, R.; Varacallo, M. StatPearls. *Biochemistry, Glycolysis, Treasure Island (FL)*; 2021.
(51) Paul, A.; Hatté, C.; Pastor, L.; Thiry, Y.; Siclet, F.; Balesdent, J. Hydrogen dynamics in soil organic matter as determined by ^{13}C and ^{2}H labeling experiments. *Biogeosciences* **2016**, *13*, 6587−6598.
(52) Kremer, K.; van Teeseling, M. C. F.; Schada von Borzyskowski, L.; Bernhardsgrütter, I.; van Spanning, R. J. M.; Gates, A. J.; Remus-Emsermann, M. N. P.; Thanbichler, M.; Erb, T. J. Dynamic metabolic rewiring enables efficient acetyl coenzyme A assimilation in *Paracoccus denitrificans*. *MBio* **2019**, 10.
(53) Martínez-Reyes, I.; Chandel, N. S. Mitochondrial TCA cycle metabolites control physiology and disease. *Nat. Commun.* **2020**, *11*, 102.
(54) Madigan, M. T.; Martinko, J. M. *Brock biology of microorganisms*; 11th ed., Pearson Prentice Hall: Upper Saddle River, NJ 2006.
(55) Typas, A.; Banzhaf, M.; Gross, C. A.; Vollmer, W. From the regulation of peptidoglycan synthesis to bacterial growth and morphology. *Nat. Rev. Microbiol.* **2011**, *10*, 123−136.
(56) Malanovic, N.; Lohner, K. Antimicrobial peptides targeting Gram-positive bacteria. *Pharmaceuticals* **2016**, *9*, 59.
(57) Apostel, C.; Dippold, M.; Kuzyakov, Y. Biochemistry of hexose and pentose transformations in soil analyzed by position-specific labeling and ^{13}C-PLFA. *Soil Biol. Biochem.* **2015**, *80*, 199−208.

(58) Gunina, A.; Dippold, M. A.; Glaser, B.; Kuzyakov, Y. Fate of low molecular weight organic substances in an arable soil: from microbial uptake to utilisation and stabilisation. *Soil Biol. Biochem.* **2014**, *77*, 304−313.
(59) Schink, S. J.; Biselli, E.; Ammar, C.; Gerland, U. Death Rate of E. coli during Starvation Is Set by Maintenance Cost and Biomass Recycling. *Cell Syst.* **2019**, *9*, 64−73.e3.
(60) Lempp, M.; Lubrano, P.; Bange, G.; Link, H. Metabolism of non-growing bacteria. *Biol. Chem.* **2020**, *401*, 1479−1485.
(61) González-Pastor, J. E.; Hobbs, E. C.; Losick, R. Cannibalism by sporulating bacteria. *Science* **2003**, *301*, 510−513.
(62) Moeller, R.; Horneck, G.; Facius, R.; Stackebrandt, E. Role of pigmentation in protecting *Bacillus* sp. endospores against environmental UV radiation. *FEMS Microbiol. Ecol.* **2005**, *51*, 231−236.
(63) Killham, K. A physiological determination of the impact of environmental stress on the activity of microbial biomass. *Environ. Pollut., Ser. A* **1985**, *38*, 283−294.
(64) Yin, Y.; Gu, J.; Wang, X.; Zhang, Y.; Zheng, W.; Chen, R.; Wang, X. Effects of rhamnolipid and Tween-80 on cellulase activities and metabolic functions of the bacterial community during chicken manure composting. *Bioresour. Technol.* **2019**, *288*, No. 121507.
(65) Bergkessel, M.; Basta, D. W.; Newman, D. K. The physiology of growth arrest: uniting molecular and environmental microbiology. *Nat. Rev. Microbiol.* **2016**, *14*, 549−562.
(66) Zhang, X.; Gillespie, A. L.; Sessions, A. L. Large D/H variations in bacterial lipids reflect central metabolic pathways. *Proc. Natl. Acad. Sci. U. S. A.* **2009**, *106*, 12580−12586.
(67) Brüggemann, N.; Gessler, A.; Kayler, Z.; Keel, S. G.; Badeck, F.; Barthel, M.; Boeckx, P.; Buchmann, N.; Brugnoli, E.; Esperschütz, J.; Gavrichkova, O.; Ghashghaie, J.; Gomez-Casanovas, N.; Keitel, C.; Knohl, A.; Kuptz, D.; Palacio, S.; Salmon, Y.; Uchida, Y.; Bahn, M. Carbon allocation and carbon isotope fluxes in the plant-soil-atmosphere continuum: a review. *Biogeosciences* **2011**, *8*, 3457−3489.
(68) Werth, M.; Kuzyakov, Y. 13C fractionation at the root−microorganisms−soil interface: A review and outlook for partitioning studies. *Soil Biol. Biochem.* **2010**, *42*, 1372−1384.
(69) Kreuzer-Martin, H. W.; Lott, M. J.; Ehleringer, J. R.; Hegg, E. L. Metabolic processes account for the majority of the intracellular water in log-phase Escherichia coli cells as revealed by hydrogen isotopes. *Biochemistry* **2006**, *45*, 13622−13630.
(70) Manzoni, S.; Schaeffer, S. M.; Katul, G.; Porporato, A.; Schimel, J. P. A theoretical analysis of microbial eco-physiological and diffusion limitations to carbon cycling in drying soils. *Soil Biol. Biochem.* **2014**, *73*, 69−83.
(71) Shimizu, K. Regulation systems of bacteria such as *Escherichia coli* in response to nutrient limitation and environmental stresses. *Metabolites* **2014**, *4*, 1−35.
(72) Chubukov, V.; Sauer, U. Environmental dependence of stationary-phase metabolism in *Bacillus subtilis* and *Escherichia coli*. *Appl. Environ. Microbiol.* **2014**, *80*, 2901−2909.
(73) Death, A.; Ferenci, T. Between feast and famine: endogenous inducer synthesis in the adaptation of *Escherichia coli* to growth with limiting carbohydrates. *J. Bacteriol.* **1994**, *176*, 5101−5107.
(74) Matin, A. Microbial regulatory mechanisms at low nutrient concentrations as studied in chemostat. *Strategies of Microbial Life in Extreme Environments*: Dahlem Konferenzen: Berlin, 1979.

https://doi.org/10.1021/acsearthspacechem.2c00085
ACS Earth Space Chem. 2022, 6, 2180−2189